Researchers Journal of Science and Technology (REJOST)
https://rejost.com.ng

Approximate delineation of groundwater yield capacity and vulnerability via secondary geo-electric indices and rock-water interaction hydrodynamic coefficients in a coastal environment

James Anthony Umoh*, Nyakno Jimmy George, Aniekan Martin Ekanem, Jewel Emem Thomas and Joseph Bassey Emah

Received: October 9, 2022 /Accepted: November 21, 2022

Abstract

Electrical geophysical method in 1-D case was used to investigate the penetration of current into the subsurface of 45 vertical electrical sounding (VES) points in the study area located within in southeastern part of Nigeria. The primary aim was to assess the groundwater yield potential index (GWYPI) and to characterize the readily available potential aquifer system in terms of vulnerability and coefficients of hydrodynamics. Resistivity meter was used to acquire VES data while WINRESIST software programme was used to estimate the primary geo-electric indices (PGI). The GPI results were used to compute the secondary geo-electric indices (SGI) used in estimating GWYPI and protective capacity (PC). Cored samples closer to the VES points were also analyzed in the laboratory and correlated with the subsurface parameters to determine the aquifer hydrodynamic parameters. At a mean depth of 114.6 m within the gamut of 39.5-290.9 m, the bulk resistivity spread between 26.3 to 3688.7 Ωm with an average of 1049.047Ωm. The thickness spread from 22.6 to 273.3m with a mean of 97.69m. The various indices realized are suggestive of the fact that the probable water repository is sustainable and vulnerable. The subsurface showed proportionally nine (9) characteristic curves, which are: (HA (1.9%), HK (13.3%), H (28.9%), KH (4.4%), AK (4.4%), K (31.1%), Q (1.9%), KQ (1.9%) and A (11.1%). The estimated anisotropy varied from 0.85 to 1.00 with a mean of 0.872. This gamut of anisotropy reflects models for groundwater yield indices and categorizes aquifers as low yield, moderate yield, high yield and very high yield. The PC was classed as poor (44.4%), weak (20.0%), moderate (28.8%) and good (6.7%) with high and moderate yield indices and good PC found near only VES 18, 27 and 28 locations. The hydrodynamic coefficients indicate that the magnitudes and distributions of pore fluid in the aquifer hydraulic units within the geologic unit are sustainable and transmissible during water-rock/soil interaction.

✉ James Umoh: jamesumoh84@yahoo.com

Department of Physics (Geophysics Research Group), Akwa Ibom State University Mkpat Enin, PMB 1162 Uyo, Nigeria

Keywords: Anisotropy; geo-electric indices; hydrodynamic coefficients; WYPI; vulnerability

Introduction

Water is a common chemical substance that is indispensable in all known forms of life. It is one of man's most abundant and critical resources, covering over 70 % of the planet's surface with approximately 975 % of the earth's surface water contained in the seas, 21 % in polar ice and glaciers, 0.3-0.8 % underground, 0.009 % in inland freshwaters such as lakes, and 0.00009 % in rivers (Eja, 2002). Water is regarded as a universal solvent existing in nature as rain, crystal clear, cold, and even free flowing. Water contains pathogens, microbes, dissolved heavy metals and bacteria that are harmful to lives of flora or fauna or both. Water in its purest form is often regarded as important to good health and many people believe that it is more fundamental than all other life necessities. The water flowing from tap may come from hundreds of miles away and the public water systems are most often supplied by surface water or groundwater. Large cities and towns usually get their water from surface water supplies or both surface and groundwater supplies (George *et al.*, 2021). Some small, rural communities rely solely on groundwater supplies, which may or may not require treatment to meet drinking water standards. Groundwater provides the most readily and sustainable source of water used by man, and the quest for potable groundwater has become more of a hydra-headed dilemma, particularly among urban people and rural communities in developing countries living very close to the river (Venkateswaran *et al.*, 2014). In the coastal terrain of Akwa Ibom State, the problem of salinisation of groundwater aquifer is due to excessive pumping of unconfined coastal aquifers, which leads to intrusion of sea water. The ingress of saltwater into freshwater makes water unsuitable and degrades its potability. Groundwater availability in any region is dependent on geology, which may change as a result of human activities or nature (George *et al.*, 2021). Its availability and suitability for use are paramount in the contemporary studies. Its quality is determined by the degree of purity after passing through the recharge and discharge processes within the geologic units (Arsene *et al.*, 2018).

The availability of groundwater as water source depends largely upon the subsurface and surface geology as well as climate, porosity and permeability of a geologic formation, which controls its ability to hold and transmit water through the aquifers (George *et al.*, 2022b). Fresh and saltwater combine at the edge of a coastal aquifer, resulting in fresh and salty water mix, which caused a balance that alters the rate of groundwater pumping that leads to flow of salty water to spaces in the sandy soil where fresh water resides. The flux in the resistivities of the Earth is attributed to some geologic parameters such as porosity, permeability, soil type, rock types and degree of saturation. The assessment of groundwater in this work employs geophysical (electrical resistivity) and laboratory methods to delineate zones of hydrogeological units for exploration of groundwater and their flow pattern (Evans *et al.*, 2010; George *et al.*, 2010). Consequently, Coastal aquifers can be highly heterogeneous in complex environments. As a result, spatial knowledge of their hydrogeological properties and development of groundwater models are essential for achieving a sustainable management of the resource. The water used in the study area is usually extracted from groundwater from boreholes, which in some cases are at risk of low or intermediate yield of iron filled water. Lithology, lineament density, geo-electric parameters (thickness and transverse resistance) are factors that influences groundwater availability, and critical study of

these factors in the aquifer system is important in order to avoid unnecessary expenses in drilling many wells (Werner *et al*., 2010). Hydraulic conductivity transmissivity and are two of the most central hydraulic data used in typifying groundwater resources because of their ability to describe an aquifer general capacity to transmit water over the entire saturated thickness for tranesmissivity and over a unit thickness for hydraulic conductivity) (Adiat *et al*., 2013). Global population expansion may contribute to water scarcity since it has made it more challenging to use and manage water resources especially when there are elevational disparities (downward) and pressure variances in the flow of groundwater (from areas of high pressure/topography to areas of low pressure/topography).

For hydrological management and planning as well as the determination of sustainable groundwater resource development, under-standing of hydrogeological properties and groundwater flow mechanisms in aquifers, detailed prognoses aquifer system are crucial. However, the preferential flow direction in all geologic materials is largely dependent on the grain sizes and flow rate of the aquifer (Thomas et al., 2020). The lithology of geological formation generally varies significantly in both horizontal and vertical planes. Consequently, the hydraulic conductivity depends on the position within the formation and varies with direction of measurement. When the hydraulic conductivity (K_h) measured in horizontal plane is significantly greater than that measured vertically, then the aquifer is said to be anisotropic in nature (Singh *et al.*, 2004). The fundamental characteristics that control groundwater hydrology are hydraulic conductivity, transmissivity, effective aquifer depth and specific yield. These parameters also serve as the input data for numerous physical models. Specifically, this work aims at assessing the groundwater yield potential index (GWYPI) of the readily available potential aquifer system in terms of vulnerability and coefficients of hydrodynamics the use of Dar-Zarrouk parameters (Transverse resistance and longitudinal conductance). The research also aims at characterizing the protective capacity of groundwater extracted in the study area as well as combining the laboratory analysis with ground-based primary and the consequent secondary geo-electric indices to typify the hydrodynamic properties for effective qualitative and quantitative hydrological assessment of the densely populated study area.

Location and Geology of study area

The study area, which is fairly low-lying according to the seemingly constant elevations measured from Geographic Positioning System (GPS) radar in Table 3, described in Figure 1 lies within the gamut of Longitudes 7°30' and 8°50'N and Latitudes 4°50' and 5°50'E and it is found in the southeastern part of Nigeria. The area has local geology predominantly called Coastal Plain sands (Benin Formation) and the terrain is mostly flat. It is accreted sediments of fluvio - lacustrine materials that are characterized by marine, deltaic, estuarine and lagoonal nature due to its location. Some of the Local Government Areas (LGAs) within the study location have moderate rising and falling terrain landscapes that are as high as 60 m and as low as 5 m above the mean sea levels according to Inim *et al*. (2020). The minor undulations spread in the study locations are caused by the gravitational effects to compensate for the features such as valleys, marshes, swamps, and ravines created by Atlantic Ocean, Qua Ibo, Imo, and Cross Rivers (George *et al*., 2022a). The climate of the study area is ideal for growing and extracting agricultural and forest products such as palm oil, cocoa, rice, rubber, cassava, yam and

lumber, amongst others (Inim *et al*., 2020). The survey area occupies nine (9) LGAs (Mkpat Enin, Eastern Obolo, Ibeno, Eket, Onna, Mbo, Esit Eket, Ikot Abasi and Nsit Ubium) shown in Figure 1.

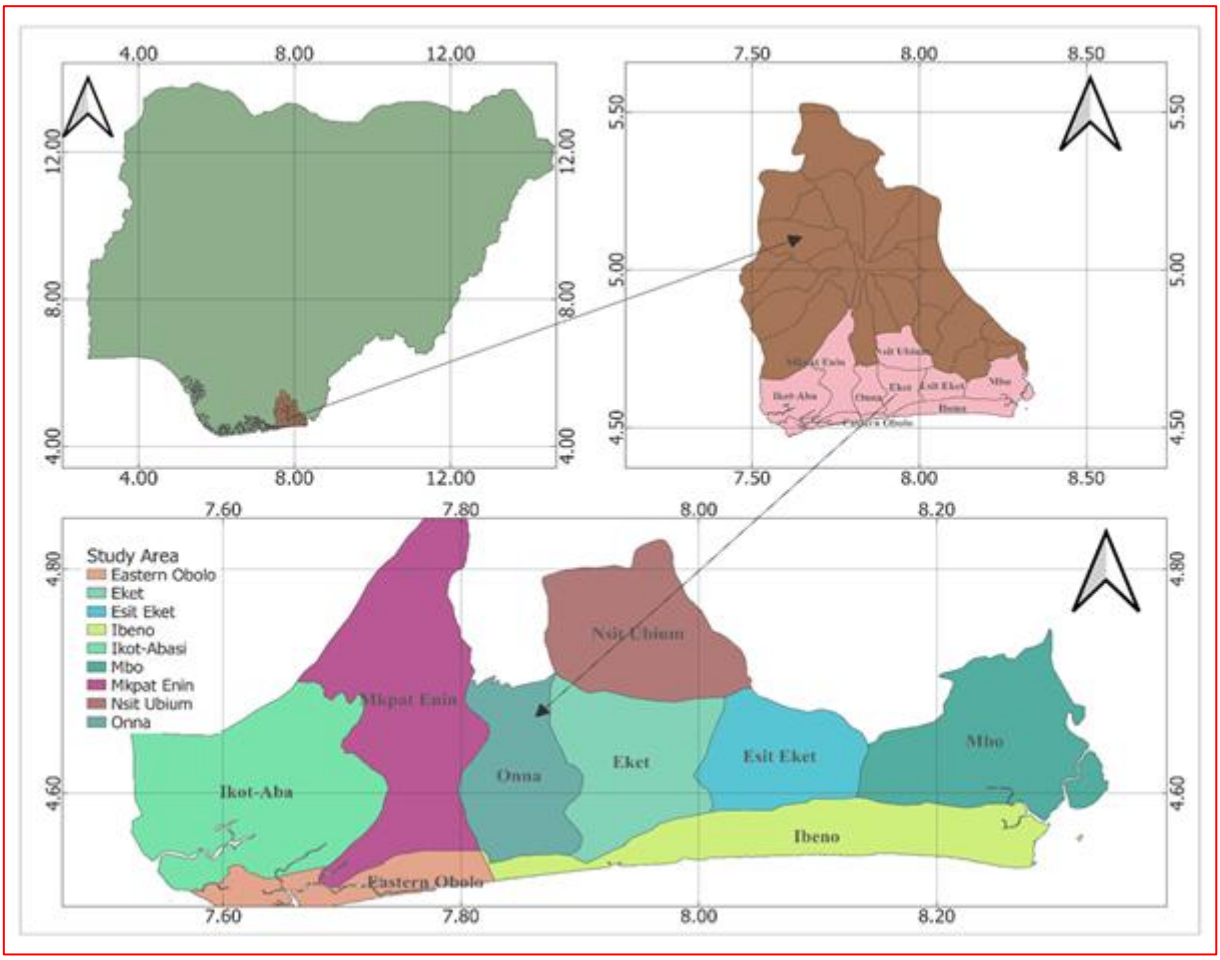

Figure 1: Map of Nigeria showing the location of Akwa Ibom State and Map of Akwa Ibom state showing the study area

All the referred LGAs fall geologically into the Coastal Plain sands (Benin Formation) shown in Figure 2. The aquifer system is made up of closed and open aquifer sands of varying pore grades, characterized by a quantum of groundwater salinity levels. The predominant geologic formation associated with reasonably high hydrodynamic coefficients (porosity and permeability) comprises the alluvium deposits and continental flood plain sands in the study area (Inim, *et al*., 2020). The Area experiences ingress of saltwater into the sedimentary aquifers under the freshwater lens, which stretches to about 5000 m away from the shoreline. The Coastal Plain sands are characterized by gravelly and medium to fine sands. The texture has pockets of thin clay horizons, lignite streaks and lenses that alternate between fine and gravelly geologic materials. The vertical and lateral spreads of the sandy aquifers are separated by thin clay/shale layers. This provoked the dominating multi-aquifer systems fraught in the area (George *et al*., 2017). With mean annual rainfall of 1.7m (66 inches), the survey area has a humid tropical climate of wet season (April to October) and a dry season (November to March). The research area is part of the Southern Nigerian Coastal Plain Sand known for prolific groundwater depositories. The area

has freshwater, freshwater swamp, coastal brackish water, dry land and beach ridge complex according to the geological survey map of Nigeria. The feel of the sediments in the study areas identifies geogenic materials of fine to coarse nature, which are disproportionately sorted, with vast thickness and inconsequential quantum of sandstones and argillites. A variety of sequences were assigned to separate aquifers of different thicknesses.

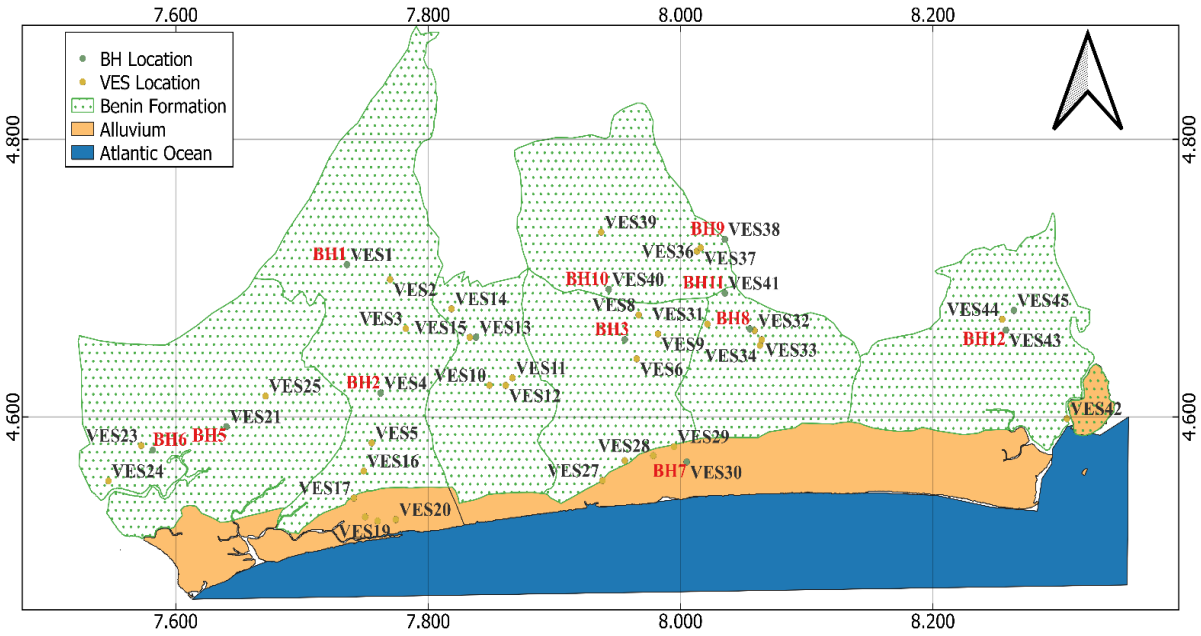

Figure 2: Study Area Geology, VES points and Borehole locations

Arenites and argillites of carbonaceous alluvial components and unconsolidated sands constitute the elevated sandy aquifer of the study area (George *et al*., 2022a). The study area is positioned at the equatorial climatic region of the Niger Delta, with high temperature of about 95 ^{0}F (35 ^{0}C) in the dry season. This instigates a shift at the lower and upper margins of the climatic conditions. From figure 1, the southernmost part of the Study area is purely made of sands that are of alluvial, lagoonal and tidal nature (Thomas *et al*., 2020). Geologically, the study location is marked by Benin Formation of Tertiary to Quaternary age. This is underlain by the paralic Agbada Formation of about 85 % of the study area and the Akata Formation, which is shally in nature. In a nutshell, the groundwater repositories of the study area are primarily sand deposits with insignificant intercalations of lignite, clay, and conglomerate. The chunk of the sands in the area is lithic arenites with size gradation spreading from fine to coarse, sub-rounded to sub-angular and poorly to moderately conjoined in their distributions.

Materials and Method

VES Techniques

Electrical resistivity technological approach is employed in integrating the hydrogeological/ geologic parameters of the study area using Schlumberger electrode configuration with electrode spacing (AB/2) for outer/current electrode separations and (MN/2) for inner/potential electrode separations. The electrodes AB and MN were gradually increased with respect to a fixed center, from 1 to 600 m and 0.25 to 60 m respectively. ABEM Terrameter SAS 1000 and its accessories were used to measure the resistance of the earth, which is believed to be varying vertically and

horizontally due to the geogenic and exogenic activities (Ibanga and George, 2016; Inim *et al.*, 2020; Thomas *et al.*, 2020). Electrical currents were injected into the ground through a set of outer/current electrode (AB/2) separations. The injected current (*I*) created a potential difference (ΔV) within the inner electrode (MN/2) separations. The ratio $\left(\frac{\Delta V}{I}\right)$ gives the apparent resistance of the earth's layer R_a. The apparent resistivity of the earth was computed using the geometric factor (G) through the expression given in Equation 1:

$$\rho_a = \pi\left[\frac{(AB/2)^2 - (MN/2)^2}{(MN)}\right]\frac{\Delta V}{I} = GR_a \quad (1)$$

where $G = \pi\left[\frac{(AB/2)^2 - (MN/2)^2}{(MN)}\right]$ and $R_a = \frac{\Delta V}{I}$.

Quality assurance in measurement was ensured by maintaining straight lines in the current and potential electrode separations. Electrodes were also made to have firm contact with the ground by making sure that one-third of the electrode penetrated the ground. Besides, the electrodes were not allowed to get in contact with grasses and measurements were not done under the power lines to avoid electromagnetic influences on the earth's electric field measured. The acquired data were manually preprocessed by plotting the apparent resistivity ρ_a against the half of the current electrode separations (AB/2) on a bi-logarithmic graph. Smoothening was done by deleting the outliers that stood out in the trend (Akpan *et al.*, 2013; George et al., 2016). The smooth results of apparent became resistivity the input data for the electronic 1-D resistivity inversion. The data (apparent resistivity and their corresponding half of current electrode separations) were inputted into the Win-Resist software programme for the final inversion. The software programme compared the field curve with the theoretical curve through curve matching procedures. Least-square inversion was achieved through iterations. The final curve in each case was associated with root-mean square error (RMSE). The electronic inversion of resistivity was constrained by ground truth data and goodness of fit realized from the curve matching results is clear evidence that the results are consistent with the geologic layers delineated (see Figure 3). From VES curves, the primary geo-electric indices (layer resistivity, thickness and depth) for each location were identified.

The secondary geo-electric parameters such as Dar Zarrouk parameters (longitudinal conductance (S) and Transverse resistance (T_r)), average vertical resistivity (ρ_T), average longitudinal resistivity (ρ_L) for a depth of *H* and anisotropic coefficient (λ) were all obtained with the following relations given in equations 2-6:

$$S = \sum_i^n \frac{h_i}{\rho_i} \quad (2)$$

$$T_r = \sum_i^n h_i \rho_i \quad (3)$$

$$\rho_t = \frac{T_r}{H} \quad (4)$$

$$\rho_L = \frac{H}{S} \quad (5)$$

$$\lambda = \sqrt{\frac{\rho_t}{\rho_L}} \quad \text{or} \quad \lambda = \frac{\sqrt{T_r S}}{H} \quad (6)$$

Laboratory measurements from aquifer samples

Porosity, Hydraulic conductivity and permeability

Aquifer materials obtained during the drilling

of boreholes in the study area close to the VES points were used to determine the porosity, hydraulic conductivity and the consequent permeability described as the transmissibility determinants during water – rock/soil interactions. The aquifer samples were satisfactorily drenched in distilled water in order to do away with any latent salt contaminations that might affect the pore system of the aquifer geo-materials and the consequent porosity therein.

The clean aquifers were desiccated with oven in order to remove the extraneous liquid within the pore system. Afterward, the bulk density (BD) for each of the aquifer materials was gauged through the aquifer weighted mass (Am)- volume equivalent (V) ratio of the dry samples as given in equation 7:

$$BD = \frac{Am}{V} \qquad (7)$$

The fairly constant aquifer/soil particle density (SPD),which ranges from 2.60 to 2.75 g/cm^3 with invariant mean of 2.65 g/cm^3 (Umoh et al., 2022) was used to calculate the aquifer pore space fraction, also known as porosity (ϕ) according to equation 8:

$$\phi = \left(1 - \frac{BD}{SPD}\right) \qquad (8)$$

The hydraulic conductivity of the aquifer samples, which is a property of rock/soil layering, was determined according to Todd (1980) from the constant flow head permeameter (CFHP) arrangement in Figure (4).

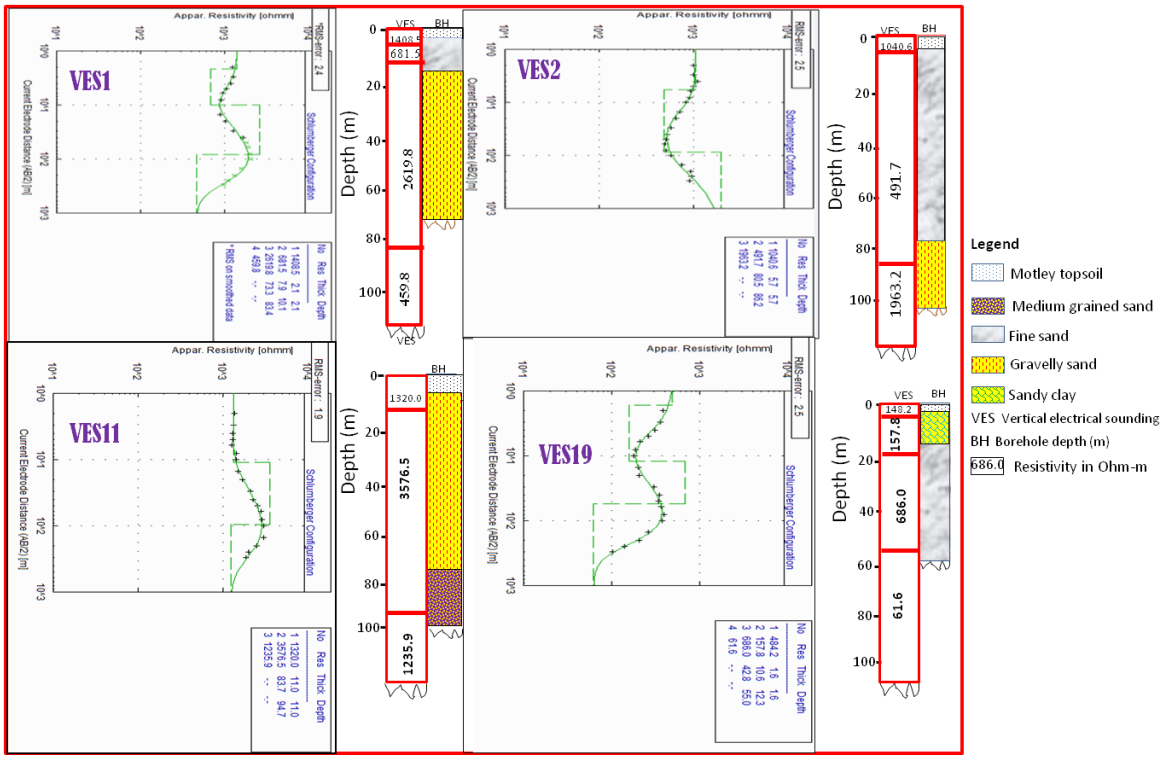

Figure 3: Sampled correlations of VES 1, 2, 11 and 19 curves with their contiguous lithological log in the study area

Steady and continuously supplied water passing through the inlet caused a continuous flow of water via the aquifer sample, which has a known area of A (Fig.4.). A stopwatch was employed in recording the duration of time (t) in which water flowing was up to 100 cm^3 mark of volume (V) in Figure 4. According to Todd (1980), different samples have different flow

rate, determined by their porosity/pore space or permeability. The CFHP made possible the estimation of the hydraulic conductivities of unconsolidated aquifer samples under the low heads. CFHP consists of aquifer sample of cross sectional area, *A* and aquifer length *L*. The aquifer sample was sandwiched with two leaky plates in a cylindrical-like tube of a constant-head differential *h*. The continuously flowing water from reservoir supply permeated into the cylinder containing the aquifer sample from the base and was collected after streaming upward through the aquifer sample as overflow (Tang et al., 2017). Based on the CFHP, hydraulic conductivity K_h,, a measure of the ease of a material medium to transmit fluid (George et al. 218; George, 2020) was gauged in m/s using equation 9 and was converted to m/day in Table 2.

$$K_h = \left(\frac{VL}{Aht}\right) \quad (9)$$

With density of water $\left(1000\,\mathrm{kg}m^{-3}\right)$, dynamic viscosity, μ_d of water given by Fetters (1994) for similar sandy materials as $\left(0.0014 kgm^{-1}s^{-1}\right)$ and acceleration due to gravity $\left(g = 9.8ms^{-2}\right)$, $K_p - K_h$ relation given in equation 10 was used to estimate the intrinsic permeability K_p in the study area.

$$K_P = \frac{K_h \mu_d}{\delta_w g} \quad (10)$$

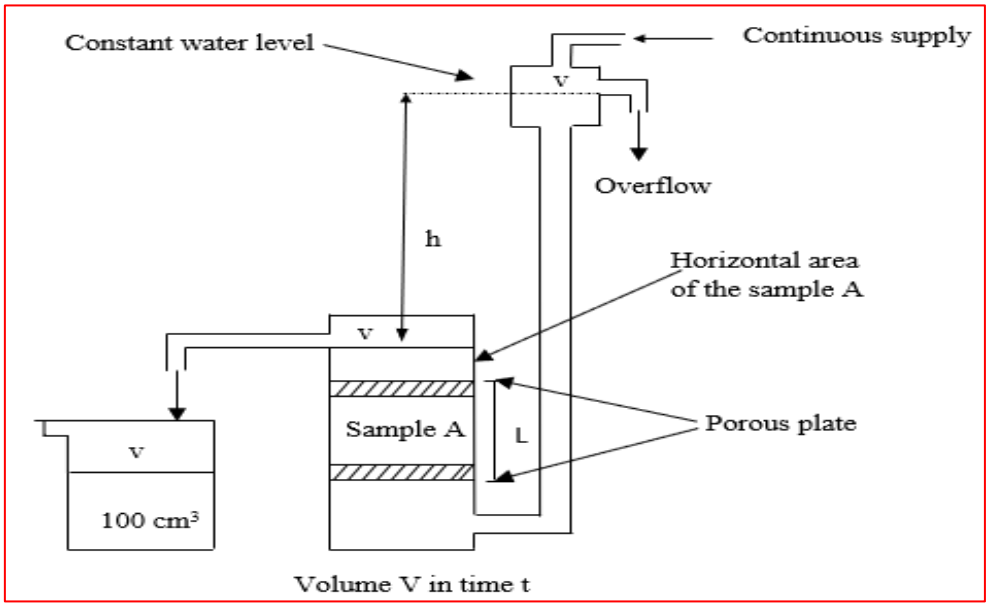

Figure 4: Constant flow head permeameter for measuring hydraulic conductivity of aquifer sample (Todd, 1980)

The water resistivity (ρ_w) for aquifer system in each location within the study area was estimated using the aquifer bulk resistivity (ρ_b) in equation 11. The parameters *m* and *a respectively* representing the average cementation factor (2.15) and pore geometry factor (0.62) were obtained from the work of George et al. (2018), which had similar geologic units.

$$\rho_w = \frac{\rho_b \phi^m}{a} = \frac{\rho_b \phi^{2.15}}{0.62} \quad (11)$$

The formation factor $\left(F = \frac{\rho_b}{\rho_w}\right)$ and the tortuosity $\left(\gamma = \sqrt{F\phi}\right)$ were determined for the aquifer to further characterize the aquifer systems. The formation factor gave the bulk-

water resistivity ratio while tortuosity gave the ratio that characterizes the convoluted pathways of fluid diffusion and electrical conduction through porous media, as well as the measure of the geometric complexity of the porous medium between the curved paths followed by a fluid in the porous medium over a straight path. These other sets of secondary geogenic parameters of aquifer systems helped in typifying the hydrodynamics of the aquifer pore system in the study area (George et al. 2015b). Vulnerability to both natural/geogenic and anthropogenic contaminations was based on one of the Dar Zarrouk parameters known as longitudinal conductance evaluated using equation 2. The lithological nature is the major factor, which decides on the protectivivity or the vulnerability coefficients defined by the longitudinal conductance during water – rock interactions in Table 1 according to Oladapo et al. (2004). Since the aquifer system is generally porous, as porosity and permeability show, the ease of transmissibility of contaminant distribution is possible within and outside and aquifer system (George et al., 2018).

According to Olubusola et al. (2018), the groundwater yield potential index (Γ), a function of the product of coefficient of anisotropy (λ) and the transverse resistance (T) was estimated in the work based on the expression given in equation 12. The classification of groundwater potential index in the area is based on Table 2, according Olubusola et al. (2018).

$$\Gamma = \lambda * T \qquad (12)$$

Results and Discussion

The interpretative 1-D resistivity sounding data of the forty five VES points from geo-electric prospection, which were constrained by the nearby ground truthing data, enabled the primary characterization of the subsurface layers penetrated by current through the identified primary geo-electric indices in the study area (Figure 3). These primary geo-electric indices (layer resistivities, thicknesses and depths) aided in the characterization of the aquifer geo-electrically and geo-hydraulically. The primary indices were combined to obtain the secondary indices such as Dar Zarrouk parameters, transverse and longitudinal resistivities, coefficients of anisotropy and groundwater yield index. The available cored samples were used to estimate the void space/porosity of the aquifer systems using the measured bulk densities and the average particle density (see equations 7 - 8). Likewise, hydraulic conductivity was experimentally determined according to Todd (1980) in equation 9 using the experimental set up in Figure 4. The consequent permeability, which depends on hydraulic conductivity, was estimated using equation 10. The estimation of these parameters gave information that reflected the dynamism of aquifer system, protectivity/vulnerability and the yield capacity during water- rock/soil interactions (Akingboye, *et al*., 2022). Despite the prolificacy of the aquifer, based on the thickness and hydrodynamic coefficients of groundwater repositories seen in porosity, formation factor, tortuosity, hydraulic conductivity and permeability, the shallowest aquifer system is greatly sensitive to drawdown and this underlines the quest for sustainability of economic aquifer system in the face of preponderant and undaunting climatic changes (Ibuot *et al*. 2017; 2019). In order to get the geo-electric indices, ohmic conduction was established between the subsurface and the quadruple Schlumberger electrodes, made up of a pair of current/outer electrodes and a pair of potential/inner electrodes (Uwa *et al*., 2019; Thomas *et al*., 2020; Ikpe *et al*., 2022; Umoh *et al*., 2022). The probing of varying earth's conductivity and the consequent apparent resistivity were assessed through the potential difference between the inner electrodes

provoked by outer electrodes (Udosen *et al*., 2018a, b; Ekanem *et al*. 2022). A Computer based analysis, which followed a manually processed apparent resistivity- half of current electrode plots of each geo-sounding point, was performed to estimate the primary geo-electric indices in Figure 3. The sample of results in Figure 3 was obtained using Win-Resist software programme, which worked iteratively to match the measured field data with the theoretical field curve in a least squared sense (Akpan *et al*., 2013; Ibuot *et al*., 2013). The validity of the results constrained by ground truths was seen in the goodness of fit measured by the Root-mean square errors (RMSE) found in general to be less than 5 % (Figure 3). This agrees with Akpan *et al*. (2013) and George *et al*. (2021), which opined that smaller RMSE suggests a good fit between the field data and the measured data and vice versa. The interpretative results as evidenced on the curves gave the primary geo-electric indices and the primary geo-electrical indices (resistivity and thickness) were conjoint in different ways to furnish the secondary geo-electric indices used primarily for estimation of groundwater yield index or capacity (Bawallah *et al*., 2018). The results from geo-electric sounding showed high and low values of resistivities with depths, indicating the heterogeneous nature of the subsurface (Obianwu *et al.*, 2011 a, b, c, d). The outcomes of geo-sounding gave three to four geological layers. In brief, the 45 VES points showed a resistivity range from 21 to 1685 Ωm and mean of 553 Ωm in layer 1. In layers 2 and 3 the respective resistivity ranged from 26 to 3689 Ωm and 45 to 3793 Ωm and mean values of 883 Ωm and 1192 Ωm were identified. The last layer resistivity ranged between 62 and 1562 Ωm with mean value of 633 Ωm. The lithological thicknesses for the first three layers varied between 0.4 to 40.0 m, 5.2 to 262.6 m and 42.8 to 237.3m respectively. Their gauged average of 8.4 m, 75.1 m and 102.0 m were respectively obtained as well for layers 1 to 3. The average values for the depths of burial for layers 1 to 3 were found to vary from 0.4 to 40.0 m, 6.9 to 265.0 m and 55.5 to 290.1 m while the calculated mean values were found to have respective values of 8.2m, 83.8m and 122.5 m. The depths and thicknesses of the last (fourth) layers were not defined by the maximum electrode current separations (see Figure 3). However, the laboratory analysis of the cored sample revealed that porosity has a strong relationship with depth. This assertion agreed with Umoh *et al.* (2022).The estimated values of the primary geo-electric indices in the study area are typical of the values obtained in the geology of Niger Delta, which is characterized by sand- beds of Benin Formation within the inferred depths (Akpan *et al*., 2020 a, b; Inim *et al*., 2020; Thomas *et al*., 2020; Ikpe *et al*., 2022; Umoh *et al*., 2022; Akpan *et al*., 2022). Although the motley topsoil is not real and their resistivity cannot be relied upon, below it, the lithological changes in the study area have resistivities reflecting gravelly/coarse sands $(>1500\,\Omega\text{m})$, medium to fine sands $(500\Omega m \le \rho < 1500\Omega\text{m})$ and fine to clayey sands $(<500\,\Omega\text{m})$. These lithofacies changes are in agreement with the ground truth data (Figure 3). The facies changes, which determined the aquifer bulk resistivities in Table 3, can be appreciated from the iso-resistivity contour map (Figure 5), which is in tandem with the vertical and horizontal textures of the soil/rock profiles at their various depths of investigations. The aquifer water resistivities, which were computed using similar average empirical constants determined by George *et al*. (2018) for similar geological textures were estimated using equation 11with the aid of fractional porosities. The result of water resistivity presented in Table 4 was contoured in Figure 6. The map shows a distribution of bulk resistivity that follows the pattern of aquifer bulk resistivities.

Table 1: Aquifer system longitudinal conductance and its protectivity capacity (Oladapo *et al*., 2004)

Longitudinal Conductance (Siemens)	Protectivity Capacity
>10	Excellent
5-10	Very good
0.8-4.9	Good
0.2-0.79	Moderate
0.1-0.19	Weak
<0.1	Poor

Table 2: Groundwater yield value range according (Olubusola *et al*., 2018)

Ground Water Yield Index (GWYI)	Yield potential
474 – 2000	Very low
2000 – 5000	Low
5000 – 10000	Moderate
10000 – 30000	High
>30000	Very high

Table 3: Geo-electrical properties of Aquifers in the Study Area

VES	Elevation (m)	Latitude (Degree)	Longitude (Degree)	Bulk Resistivity Ωm	No. of Layers	Depth (m)	Thickness (m)
1	30	4.7098	7.7355	2619.8	4	83.4	73.3
2	29	4.6990	7.7698	491.7	3	86.2	80
3	34	4.6636	7.7822	80.7	3	90.9	54.7
4	26	4.6171	7.7622	266.2	4	65.3	56.2
5	17	4.5812	7.7553	419.7	4	165.4	151.2
6	19	4.6418	7.9652	1300.7	3	51.2	49.8
7	31	4.6557	7.9558	1301.7	4	87.1	72.2
8	20	4.6735	7.9668	970.5	3	250	247.7
9	30	4.6598	7.9821	1502.6	4	109.1	93.9
10	30	4.6227	7.8485	3688.7	3	108	103.8
11	21	4.6281	7.8667	3576.5	3	94.7	83.7
12	14	4.6226	7.8614	2560.6	3	136	136.2
13	22	4.6574	7.8379	1810.5	4	90.5	79.5
14	25	4.6779	7.8184	85.1	3	265	22.6
15	23	4.6573	7.8329	2984.5	4	245.4	213.1
16	17	4.5609	7.7489	114.1	3	73.3	63.1
17	16	4.5415	7.7411	558.8	3	239	208.6
18	17	4.5279	7.7500	26.3	3	66.5	65.6
19	13	4.5249	7.7598	686	4	55	42.8
20	17	4.5259	7.7742	153.9	3	40	40
21	15	4.5930	7.6401	1864.2	3	55.3	51.7
22	10	4.5761	7.5817	182.5	3	80.2	76
23	10	4.5793	7.5726	53.3	3	39.5	29.5

24	17	4.5538	7.5466	878.9	3	101	85.2
25	24	4.6150	7.6711	1831.4	4	99.3	63
26	8	4.5684	7.9558	211.5	3	80.1	79.2
27	7	4.5541	7.9381	39.3	3	176	173.3
28	15	4.5720	7.9783	226.6	3	182	170
29	8	4.5785	7.9948	235	3	97.9	95
30	8	4.5674	8.0048	100.1	3	122	118.7
31	21	4.6669	8.0212	1076.6	3	136	119.6
32	36	4.6622	8.0586	1179.9	3	89.4	81.5
33	40	4.6556	8.0644	238.8	4	91.4	66.1
34	40	4.6516	8.0629	1469.5	4	290.9	273.3
35	38	4.6634	8.0549	1027.9	3	54.5	50.7
36	35	4.7193	8.0130	862.7	3	64.4	62.3
37	35	4.7218	8.0159	728.1	4	126.5	104.2
38	34	4.7280	8.0351	1000.7	3	89.7	76.5
39	35	4.7331	7.9371	993.4	3	124	112.4
40	40	4.6919	7.9430	622.5	4	113.7	89.4
41	23	4.6892	8.0351	300.2	3	57.2	52.7
42	16	4.5987	8.3061	2204.9	3	89.9	78.8
43	30	4.6626	8.2578	2092.3	3	197	159.9
44	27	4.6703	8.2549	735.7	3	105	104.1
45	17	4.6767	8.2640	1852.5	4	91.9	85.1

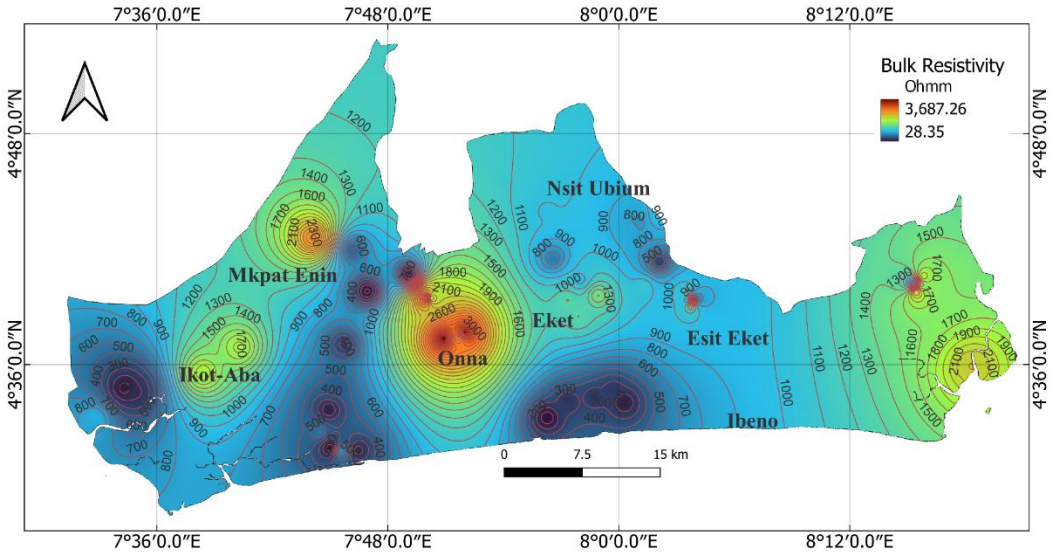

Figure 5: Bulk resistivity contour map of the aquifer in the study area

Table 4: Summary of aquifer secondary geo-electrical and hydraulic indices

VES	S (Ω^{-1})	T (Ωm)	(ϕ)	K (m/day)	K_p (mD)	ρ_w (Ωm)	F	ρ_L (Ωm)	ρ_t (Ωm)	(γ)	(λ)
1	0.028	192031.3	0.41	3.45E-05	4.99	609.7	4.30	2981	2303	1.321	0.879
2	0.163	39336.0	0.44	3.05E-05	4.42	135.2	3.64	530	456	1.264	0.928
3	0.678	4414.3	0.39	2.16E-05	3.13	17.5	4.62	134	49	1.348	0.602
4	0.211	14960.4	0.37	3.57E-05	5.17	50.3	5.30	309	229	1.398	0.861
5	0.360	63458.6	0.42	2.25E-05	3.26	106.5	3.94	459	384	1.291	0.914
6	0.038	64774.9	0.42	1.66E-05	2.40	330.6	3.93	1337	1265	1.291	0.973
7	0.055	93982.7	0.40	1.65E-05	2.38	291.5	4.47	1570	1079	1.335	0.829
8	0.255	240392.9	0.43	3.21E-05	4.65	252.8	3.84	980	962	1.282	0.991
9	0.062	141094.1	0.40	2.80E-05	4.05	334.5	4.49	1746	1293	1.337	0.861
10	0.028	382887.1	0.39	2.09E-05	3.02	791.4	4.66	3838	3545	1.351	0.961
11	0.023	299353.1	0.43	1.29E-05	1.86	938.8	3.81	4047	3161	1.280	0.884
12	0.053	348753.7	0.40	3.21E-05	4.64	566.7	4.52	2557	2564	1.339	1.001
13	0.044	143934.8	0.43	3.26E-05	4.72	475.3	3.81	2061	1590	1.280	0.878
14	0.266	1923.3	0.40	1.75E-05	2.53	18.7	4.56	998	7	1.343	0.085
15	0.071	635997.0	0.39	9.92E-06	1.44	627.0	4.76	3437	2592	1.358	0.868
16	0.553	7199.7	0.42	3.98E-05	5.76	28.5	4.01	133	98	1.297	0.861
17	0.373	116565.7	0.42	3.89E-05	5.63	137.9	4.05	640	488	1.301	0.873
18	2.494	1725.3	0.42	3.99E-05	5.78	6.6	4.00	27	26	1.296	0.986
19	0.062	29360.8	0.42	3.86E-05	5.59	168.7	4.07	882	534	1.302	0.778
20	0.260	6156.0	0.42	3.97E-05	5.75	38.4	4.01	154	154	1.297	1.000
21	0.028	96379.1	0.41	3.63E-05	5.25	444.7	4.19	1994	1743	1.313	0.935
22	0.416	13870.0	0.42	3.96E-05	5.74	45.5	4.01	193	173	1.298	0.948
23	0.553	1572.4	0.42	3.99E-05	5.77	13.3	4.00	71	40	1.296	0.747
24	0.097	74882.3	0.42	3.82E-05	5.54	215.1	4.09	1042	741	1.304	0.844
25	0.034	115378.2	0.41	3.63E-05	5.26	437.2	4.19	2887	1162	1.312	0.634
26	0.374	16750.8	0.45	3.11E-05	4.51	60.9	3.47	214	209	1.248	0.989
27	4.410	6810.7	0.42	3.14E-05	4.55	9.8	4.00	40	39	1.296	0.985
28	0.750	38522.0	0.43	2.22E-05	3.21	58.9	3.85	243	212	1.283	0.934
29	0.404	22325.0	0.42	3.95E-05	5.72	60.0	3.92	242	228	1.289	0.970
30	1.186	11881.9	0.46	3.98E-05	5.76	29.8	3.36	103	97	1.237	0.973
31	0.111	128761.4	0.42	3.78E-05	5.48	262.1	4.11	1224	947	1.306	0.879

32	0.069	96161.9	0.41	3.76E-05	5.45	286.5	4.12	1294	1076	1.307	0.912
33	0.277	15784.7	0.42	3.95E-05	5.72	59.4	4.02	330	173	1.298	0.723
34	0.186	401614.4	0.41	3.71E-05	5.36	354.2	4.15	1564	1381	1.309	0.939
35	0.049	52114.5	0.42	3.79E-05	5.49	250.6	4.10	1105	956	1.305	0.930
36	0.072	53746.2	0.42	3.83E-05	5.54	211.2	4.08	892	835	1.304	0.967
37	0.143	75868.0	0.42	3.85E-05	5.58	178.9	4.07	884	600	1.302	0.824
38	0.076	76553.6	0.42	3.80E-05	5.50	244.1	4.10	1173	853	1.305	0.853
39	0.113	111658.2	0.42	3.80E-05	5.50	242.4	4.10	1096	900	1.305	0.906
40	0.144	55651.5	0.42	3.88E-05	5.61	153.3	4.06	792	489	1.302	0.786
41	0.176	15820.5	0.42	3.94E-05	5.70	74.6	4.03	326	277	1.299	0.921
42	0.036	173746.1	0.41	3.56E-05	5.15	521.3	4.23	2515	1933	1.316	0.877
43	0.076	334558.8	0.41	3.58E-05	5.18	496.1	4.22	2578	1698	1.315	0.812
44	0.141	76586.4	0.42	3.85E-05	5.58	180.7	4.07	742	729	1.303	0.991
45	0.046	157647.8	0.41	3.63E-05	5.25	442.0	4.19	2001	1715	1.313	0.926

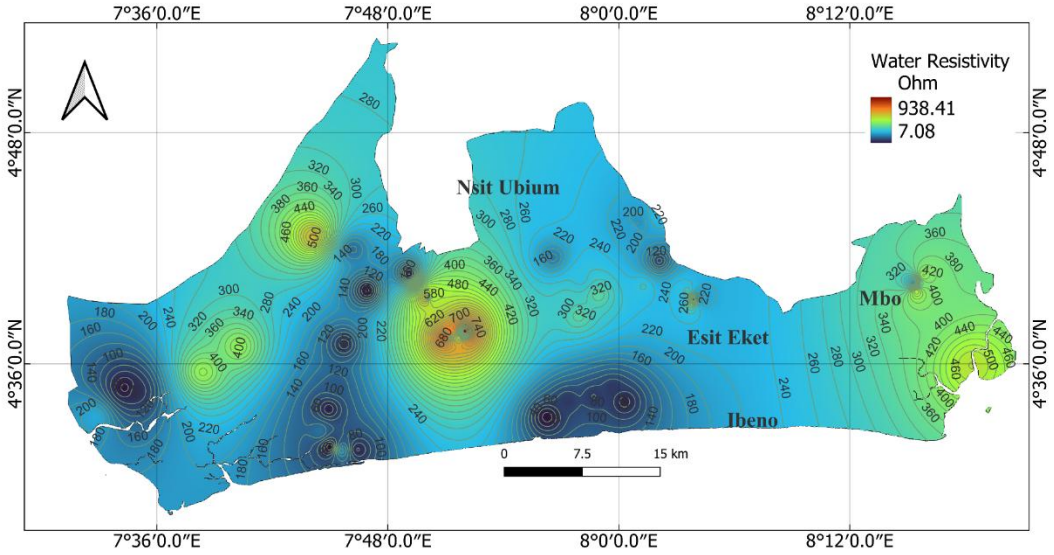

Figure 6: Water resistivity contour map of the aquifer in the study area

The two contours show the distribution of electrical facies in the study area. The depth and thickness of aquifer in Table 3, determined from the VES curves (e.g. Figure 3), gave information about the distribution of aquifer. The distribution of their contours (Figures 7 and 8) shows that as the depth increases, thickness also increases. This result agrees with the finding of George *et al.* (2021) and Umoh *et al*. (2022). The thickness of the aquifer was used in determining the Dar zarrouk parameters displayed in Figures 9 and 10 for transverse resistance and longitudinal conductance respectively. The distributions of transverse resistance and longitudinal conductance contour maps are respectively reminiscent of

the aquifer potential and its protection (Table 5) (Ekanem *et al*., 2022). The results indicate that the area is generally prolific but slightly protected from contaminants (Oladapo *et al*., 2004) as the values of longitudinal conductance show massively poor to marginally excellent protectivity (Ikpe *et al*., 2022). The longitudinal conductance exaggerates the degree of susceptibility to contamination in the study area as it ranged from 0.234 to 4.410S with a mean value of 0.357S. The hotspot of protection is shown at VES points 18 and 27, which showed very high values of longitudinal conductance. The protective capacity as estimated from the longitudinal conductance revealed poor, weak, moderate and good classes of protection respectively representing 44.4 %, 17.78 %, 31.1 % and 6.67 % in the study area (Table 5).

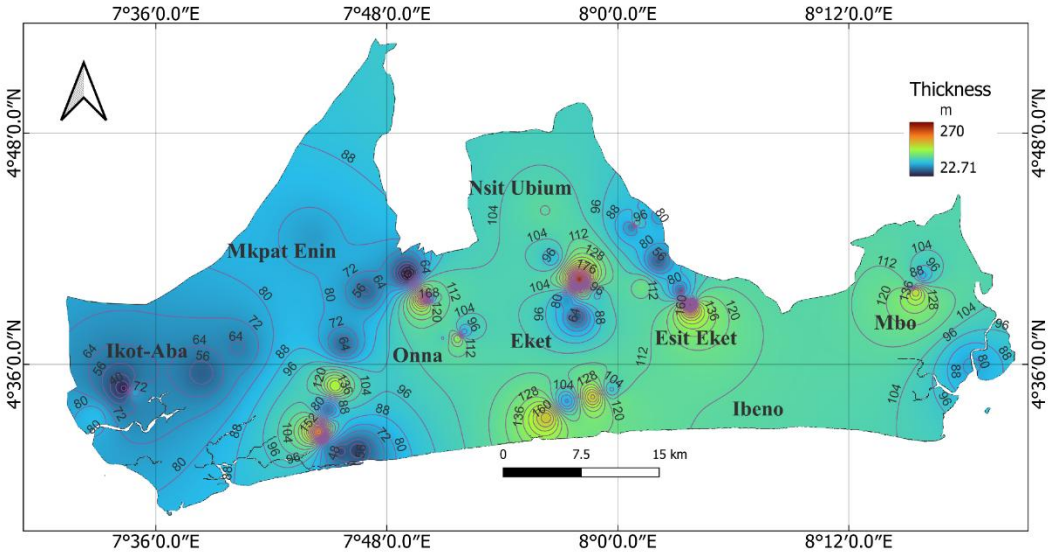

Figure 7: Thickness contour map of the aquifer in the study area

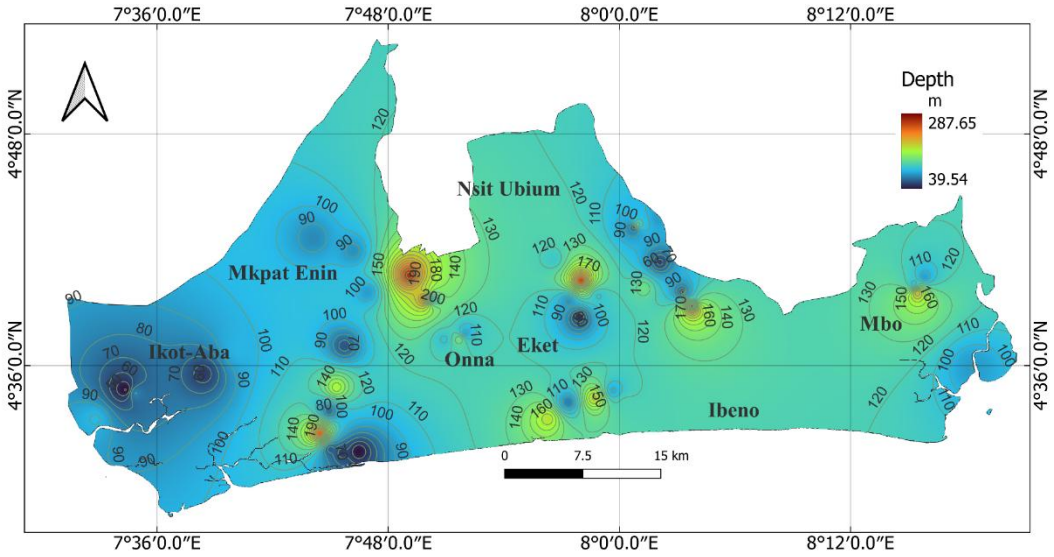

Figure 8: Depth contour map of the aquifer in the study area

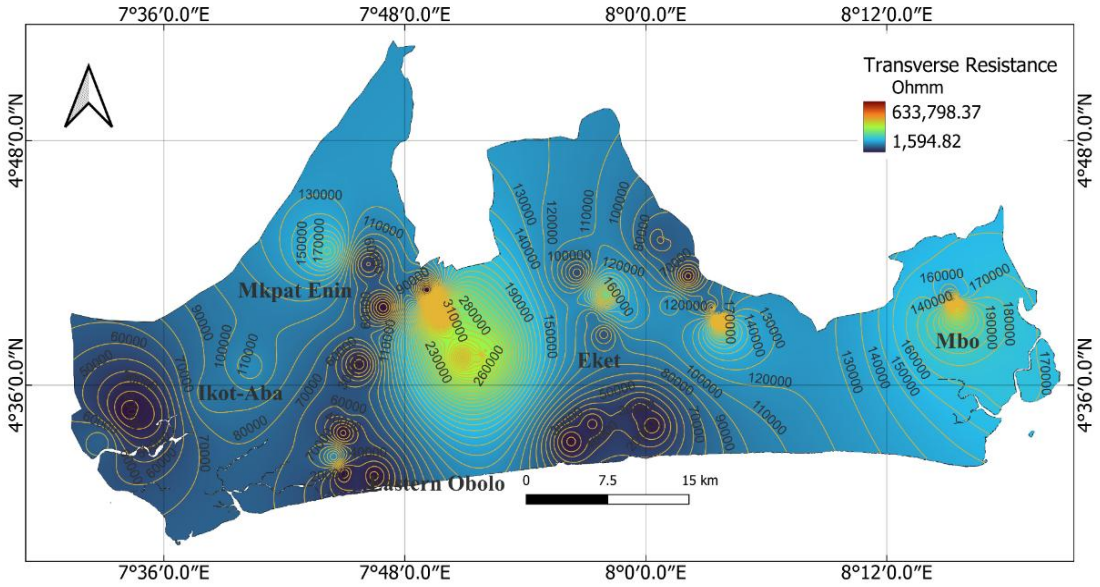

Figure 9: Transverse Resistance contour map of the aquifer in the study area

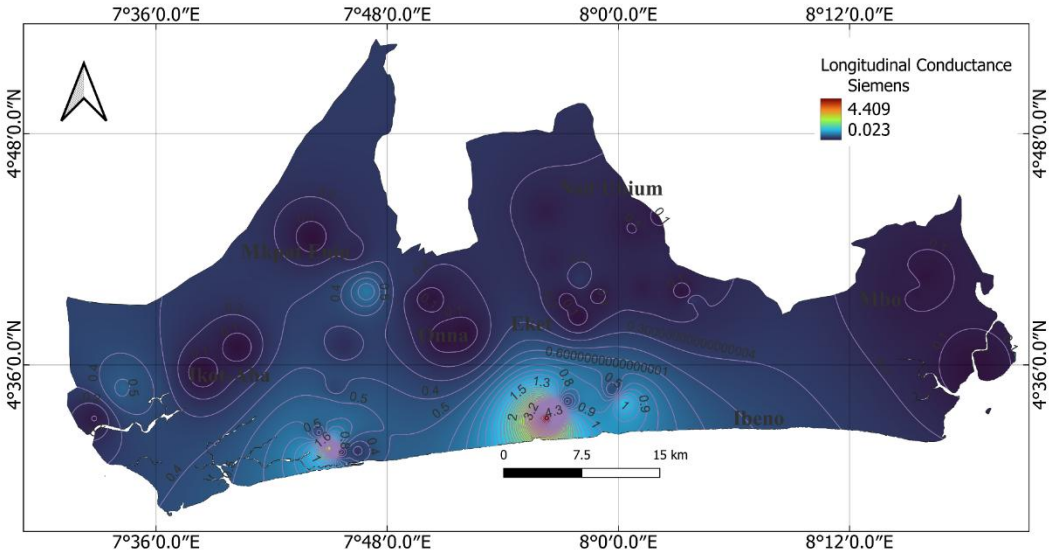

Figure 10: Longitudinal conductance contour map of the aquifer in the study area

The coefficient of anisotropy, also obtained through thicknesses and depths is displayed in Figure 11. For the accurate resolution of flow and transport issues in subsurface systems, knowledge of anisotropy, which affects fluid flow direction, is crucial. The principal lines of anisotropy line up with the spatial directions where the maximum and minimum values of hydraulic conductivity occur. Their distribution on the geo-reference map indicates that the study area has massively high potential yield index (Figure 12) but marginal protection based on its indices and the values of transverse resistance shown in Figure 9. The results indicate that why groundwater potential yield is excellent according to values obtained using equation 12 and the classification by Olubusola *et al*. (2018) in Table 2, protection is greatly poor within the depths of investigation considered. The findings from Table 5, revealed nine (9) basic curves type (A, H, K, Q, HA, HK, KH, AK, and KQ), with the Curve type A in VES 28 reflecting good protective capacity and very high yield index.

Table 5: Curve type, Protective capacity and Groundwater Yield Index of the aquifers

VES	Groundwater Yield Index	Groundwater Yield Potential	Curve type	Protective Capacity
1	168775.70	Very High Yield	HK	Poor
2	36506.73	Very High Yield	H	Weak
3	2656.34	Low Yield	H	Moderate
4	12875.60	High Yield	KH	Moderate
5	58010.56	Very High Yield	HA	Moderate
6	63003.67	Very High Yield	K	Poor
7	77905.33	Very High Yield	AK	Poor
8	238181.20	Very High Yield	K	Moderate
9	121436.70	Very High Yield	HK	Poor
10	367997.00	Very High Yield	K	Poor
11	264581.30	Very High Yield	K	Poor
12	349266.60	Very High Yield	K	Poor
13	126439.90	Very High Yield	HK	Poor
14	164.02	Very Low Yield	H	Moderate
15	552285.90	Very High Yield	AK	Poor
16	6197.84	Moderate Yield	H	Moderate
17	101738.90	Very High Yield	K	Moderate
18	1701.93	Low Yield	H	Good
19	22848.04	High Yield	HK	Poor
20	6156.00	Moderate Yield	A	Moderate
21	90104.91	Very High Yield	K	Poor
22	13143.64	High Yield	H	Moderate
23	1174.29	Very Low Yield	H	Moderate
24	63168.02	Very High Yield	Q	Poor
25	73200.67	Very High Yield	HK	Poor
26	16562.59	High Yield	A	Moderate
27	6706.21	Moderate Yield	H	Good
28	35982.09	Very High Yield	A	Good
29	21663.69	High Yield	H	Moderate
30	11560.48	High Yield	H	Weak

31	113234.30	High Yield	K	Weak
32	87664.33	Very High Yield	K	Poor
33	11415.40	High Yield	H	Moderate
34	377315.90	Very High Yield	HK	Weak
35	48480.86	Very High Yield	K	Poor
36	51993.62	Very High Yield	K	Poor
37	62493.66	Very High Yield	KQ	Weak
38	65288.14	Very High Yield	K	Poor
39	101212.70	Very High Yield	A	Weak
40	43757.64	Very High Yield	KH	Weak
41	14575.92	High Yield	H	Weak
42	152293.60	Very High Yield	K	Poor
43	271553.00	Very High Yield	K	Poor
44	75929.92	Very High Yield	A	Moderate
45	145982.80	Very High Yield	H	Poor

The positively related hydrodynamic parameters (hydraulic conductivities and permeability) with void space in Table 4 were estimated with the aid of cored samples that were close to VES the points. The distributions in the contour maps of Figures 13 and 14 respectively depict the hydraulic conductivity and permeability in the study area. The spread of hydraulic conductivity and permeability reflect a linear relationship (Figure 15) and the distribution of void space and high rate of water flow within the aquifer pores in the area (Ekanem *et al*., 2020). The curve frequency distribution chart in Figure 16 shows that there is no specific relationship of curve type with GWYPI and protection during water-rock/soil interactions. However, thickness size and the texture of the aquifer overlying layers determine the protection/vulnerability while the product of coefficient of anisotropy and transverse resistance of the aquifer determine its GWYPI (Bawallah et al., 2018; Akingboye *et al*., 2022). Again, the ratio of the pore system conductivity to that of its bulk equivalent is known as the formation factor, which describes the diffusion of ionic species in porous materials. All of the VES locations in the research area have an average value of formation factor, except those around Eket, Esit Eket, and Ibeno, which show relatively low levels of formation factor (Figure 17). This may be attributed to high ionic content of the pore water system caused by the recharging rivers. According to the result, formation factor increases near Onna and Mkpat Enin, with range and average values of 3.36 to 5.29 and 4.12 respectively. The fairly constant formation factor gave rise to fairly constant tortuosity in Figure 18. The average value of aquifer turtorsity in the study area is 1.30 with range between 1.23 and 1.39. Generally, the study area has an average value of turtorsity for all the VES points, excerpt in areas around Eket, Esit Eket and Ibeno that indicates relatively low values while areas around Onna and Mkpat Enin have higher turtorsity. The value of

tortuosity reflects the transport characteristics of porous media like soil/rock during interaction with water and is a crucial metric for flow direction. Contrary to other common microstructural characteristics, tortuosity has a variety of definitions and methods of assessment, which in this case can be used to characterize the hydraulic flow units with the geological units (Umoh *et al*., 2022).

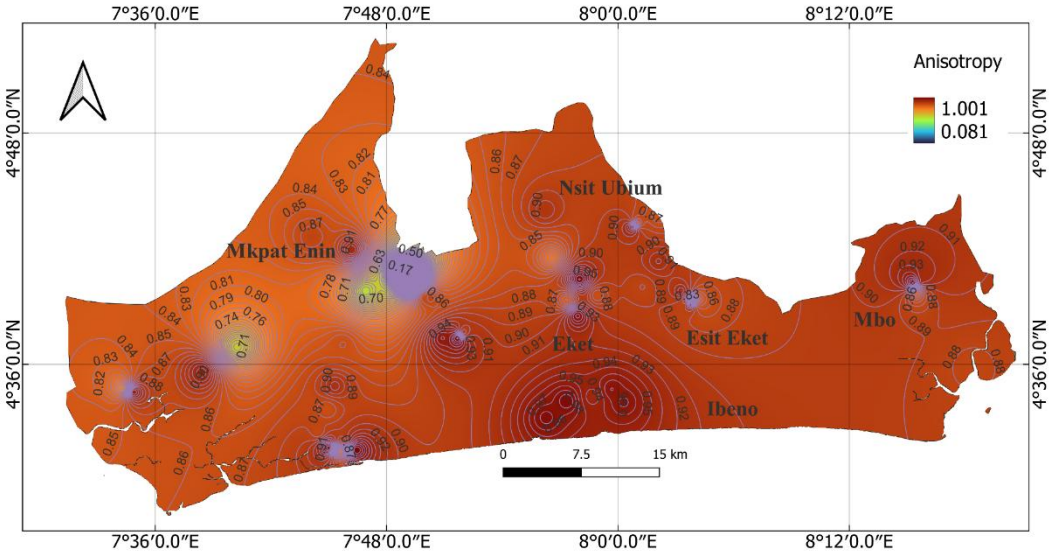

Figure 11: Anisotropy contour map of the aquifer in the study area

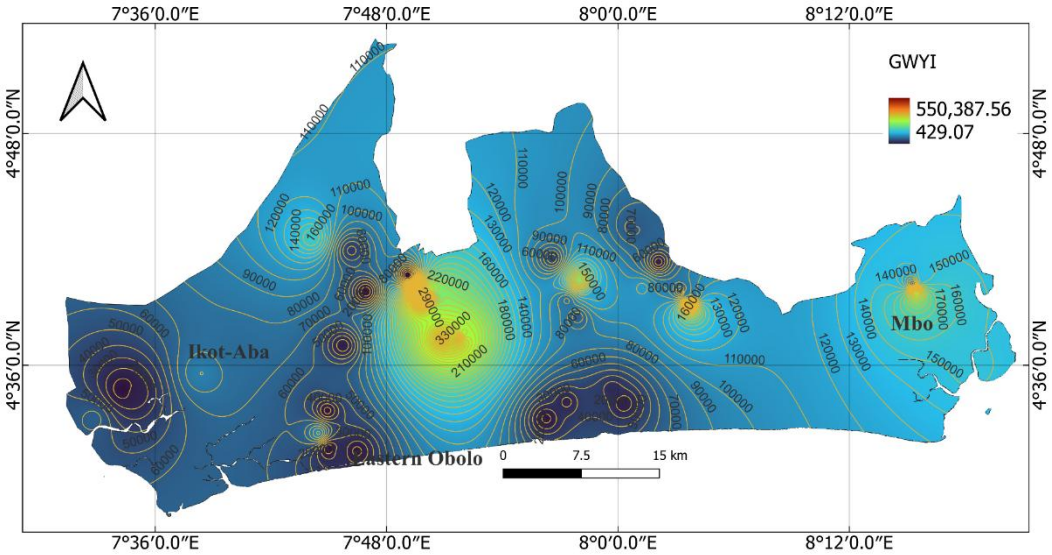

Figure 12: Aquifer groundwater yield index contour map of the study area

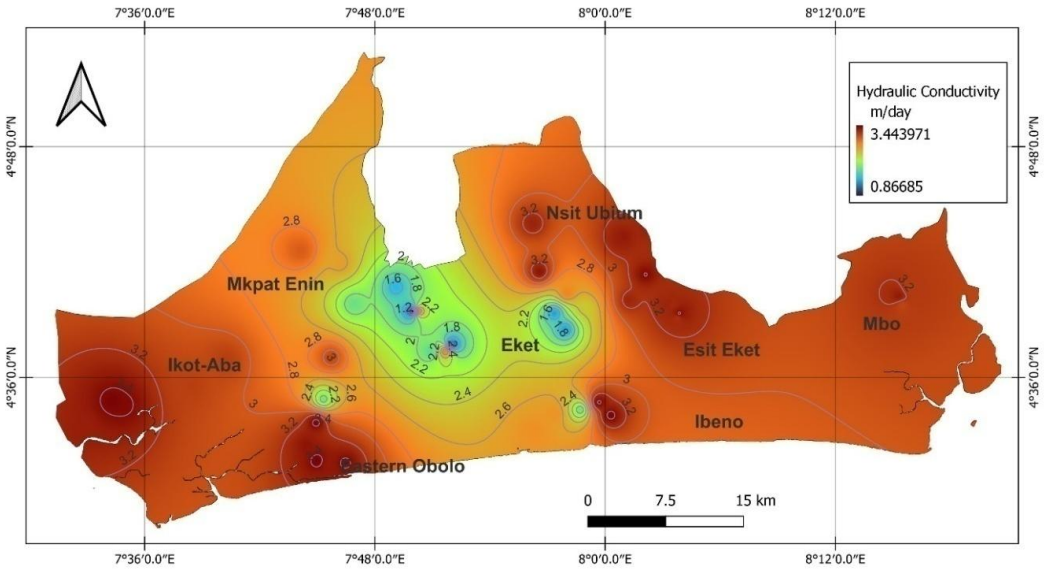

Figure 13: Hydraulic Conductivity contour map of the aquifer in the study area

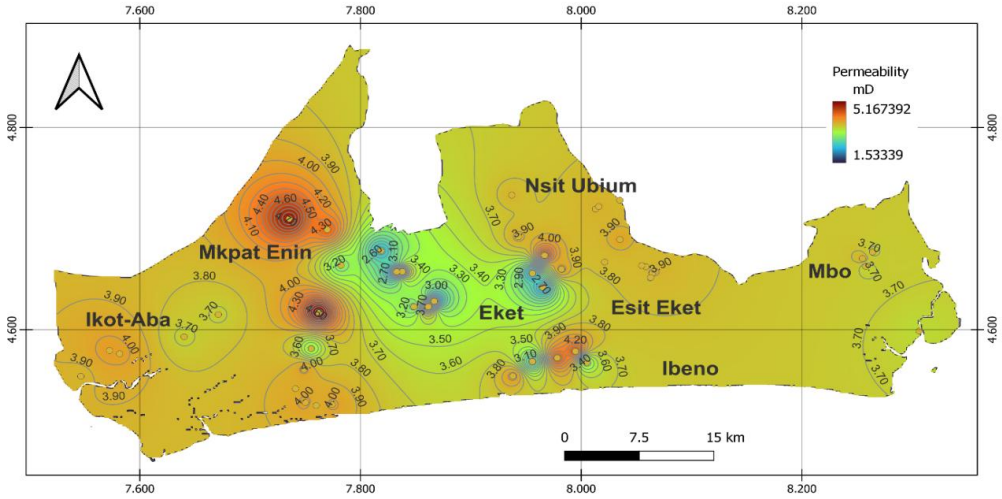

Figure 14: Permeability contour map of the aquifer in the study area

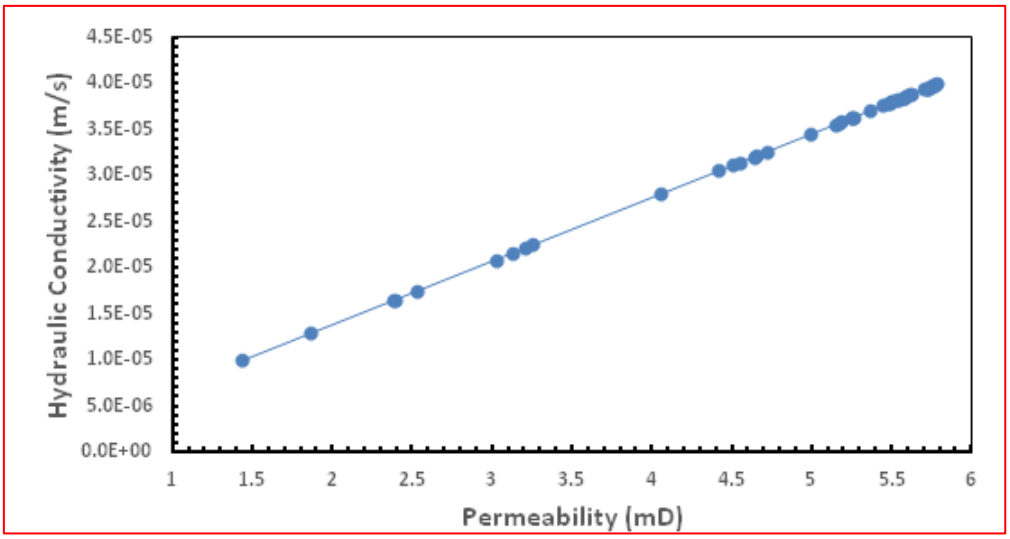

Figure 15: Plot of Hydraulic Conductivity against Permeability

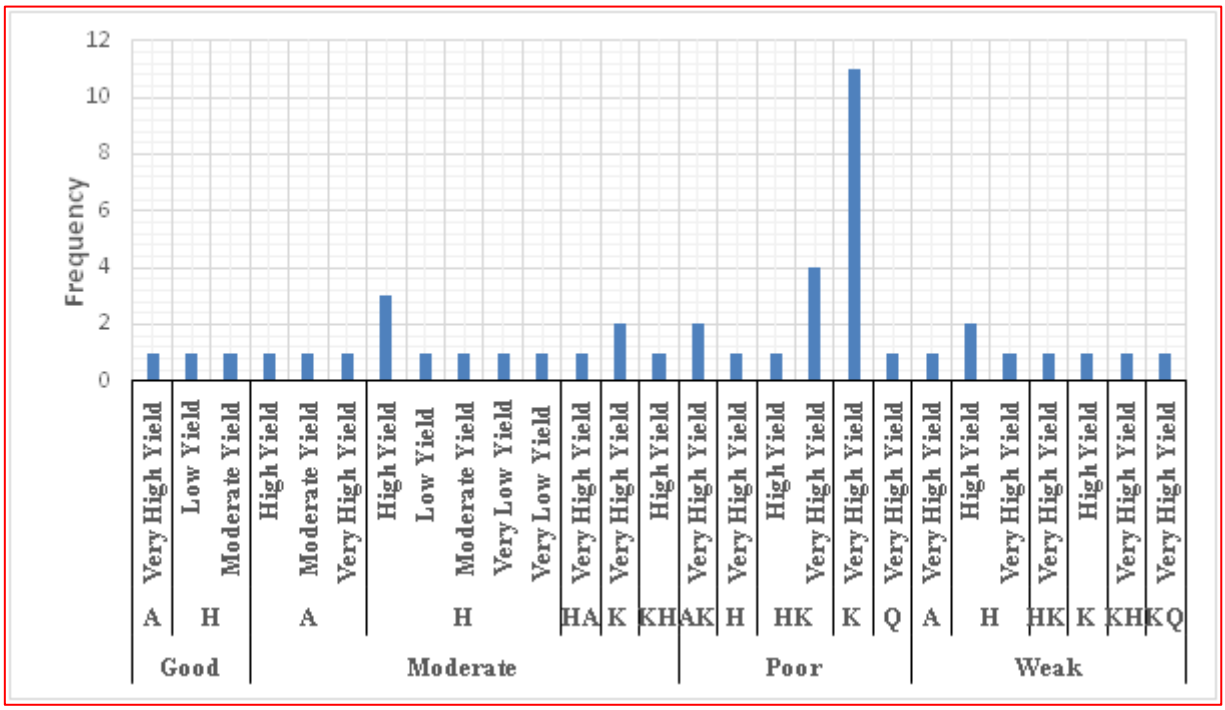

Figure 16: Multiple histograms for groundwater yield potential, curve type and protective capacity of the aquifers in the study area

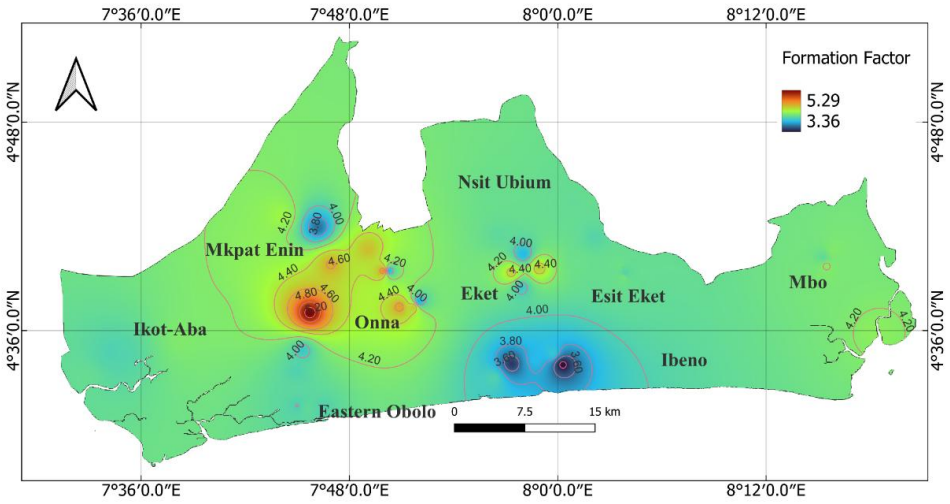

Figure 17: Formation factor contour map of the aquifer in the study area

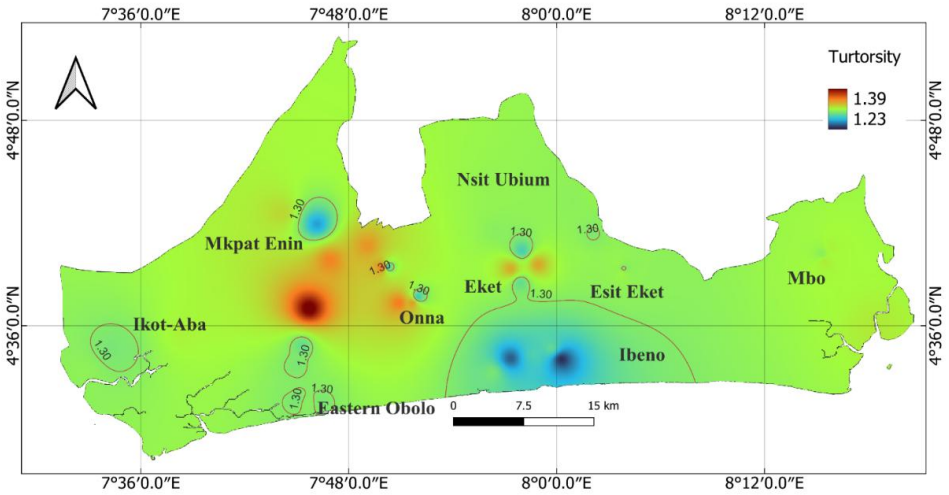

Figure 18: Turtorsity contour map of the aquifer in the study area

Conclusion

In the face of daunting climatic changes and challenges, the need to investigate or evaluate using integrated technique, the sustainability, protectivity and delineability of new aquifer systems for massive exploits is paramount. In this work, the prospection of the GWYPI and the characterization of the readily available potential aquifer system in terms of vulnerability and coefficients of hydrodynamics have been identified for the hydro-geo-resource. The groundwater system in the study area is sustainable and vulnerable based on the GWPYI and the longitudinal conductance. The study also revealed that the aquifer system assessed is highly transmissible based on the inferred hydrodynamic coefficients such as void space/porosity, hydraulic conductivity and permeability. The study area is by the findings in this work classed in terms of GWPYI as low yield, moderate yield, high yield and very high yield as well as good, moderate, weak and poor protective capacity according to longitudinal conductance. The study reveals nine (9) basic curves types (A, H, K, Q, HA, HK, KH, AK, and KQ), with the curve type A in VES 28 showing the best aquifer in the study area with a good protective capacity and very high yield index. The laboratory analysis of the cored sample also revealed that porosity has a strong relationship with depth and this is analogous with Umoh *et al*. (2022). In conclusion, the result shows that 44.4 % of the study area has poor protective capacity; 20 % has weak protective capacity; 28.8 % has moderate protective capacity and 6.67 % has good protective capacity, with moderate and good protective capacities found at VES points 18 and 27 only. The Contour map of the study area shows that the central part of the area around Onna, has the highest yield index, and some locations in Mbo, Esit Eket and Eket while low yield index is principally found in the South-western part of the study area. The result obtained in this work can be used as guide in groundwater resource monitoring and management mostly now that the climatic change is highly unpredictable..

Funding: The project was funded by the authors

Compliance with ethical standards

Conflict of interest: The authors declare that they have no known competing financial interests or personal relationships that could have appeared to influence the work reported in this paper.

Human and animal rights: This article does not contain studies with human or animal subjects.

References

Adiat KAN, Nawawi MNM, Abdullah K (2013). Application of multi-criteria decision analysis to geoelectric and geologic parameters for spatial prediction of groundwater resources potential and aquifer evaluation. *Pure Appl Geophys*, 170: 453–471

Akingboye, AS, Bery, A.A., Kayode, JS, Ogunyele, AC, Adeola, AO, Omojola, OO, Adesida, AS (2022). Groundwater-yielding capacity, water – rock interaction and vulnerability assessment of typical gneissic hydrogeologic units using geoelectrohydraulic method. *Acta Geophys*. https://doi.org/10.1007/s11600-022-00930-4

Akpan A.S., Okeke, F.N., Obiora D.N., and George N.J. (2020a). Modelling and mapping hydrocarbon saturated sand reservoir using Poisson's impedance (PI) inversion: a case study of Bonna field, Niger Delta swamp depobelt, Nigeria, *Journal of Petroleum Exploration and Production Technology*, Germany, 11, 117 – 132, https://doi.org/10.1007/s13202-020-01027-8

Akpan, A. E., Ugbaja, A. N., and George, N. J. (2013). Integrated geophysical, geochemical and hydrogeological investigation of shallow groundwater resources in parts of the Ikom- Mamfe Embayment and the adjoining areas in Cross River State, Nigeria. *Environmental Earth Sciences*, 70(3), 1435–1456. doi: 10.1007/s12665-013-2232-3.

Akpan, A.S., Obiora D.N., Okeke F.N., Ibuot J.C and George N.J. (2020b). Influence of wavelet phase rotation on post stack model based seismic inversion: A case study of X-field, Niger Delta, Nigeria, *Journal of Petroleum and Gas Engineering*, United Kingdom, 11(1), 57-67, DOI: 10.5897/JPGE2019.0320.

Akpan, MJ, George, NJ, Ekanem, AM, Ekong, UN (2022). Petrophysical appraisal and 3D structural interpretation of reservoirs in an Onshore Niger Delta Field, Southeastern Nigeria, *International Journal of Energy and Water Resources*, https://doi.org/10.1007/s42108-022-00218-9

Arsène, M, Bidichael, WWE, Daniel, G Ndougsa-Mbarga T, Kuiate, K, Ngoh JD (2018). Hydrogeophysical Investigation for Groundwater Resources from Electrical Resistivity Tomography and Self-Potential Data in the Méiganga Area, Adamawa, Cameroon, *International Journal of Geophysics*, vol. 2018, Article ID 2697585, 14 pages, https://doi.org/10.1155/2018/2697585

Bawallah, MA, Adebayo, OA, S O Ilugbo, SO, Ozegin, KO, Olasunkanmi , N, Ali, MH (2018). Evaluation of Groundwater Yield Capacity Using Dar-zarrouk Parameter of Central Kwara State, Southwestern Nigeria, Asian Journal of Geological Research1(1): 1-13, DOI: 10.9734/AJOGER/2018/42053

Ekanem A.M., **George N.J.**, Thomas, J.E. and Nathaniel E. U. (2020). Empirical Relations Between Aquifer Geohydraulic–Geoelectric Properties Derived from Surficial Resistivity Measurements in Parts of Akwa Ibom State, Southern Nigeria. *Natural Resources Research*, Switzerland, 29 (4):2635-2646, DOI 10.1007/s11053-

019-09606-1.

Ekanem AM, Akpan AE, George NJ, Thomas JE (2021). Appraisal of protectivity and corrosivity of surficial hydrogeological units via geo-sounding measurements. *Environ Monit. Assess*. 13; 193(11):718. doi: 10.1007/s10661-021-09518-9. PMID: 34642861.

Ekanem, KR, George, NJ, Ekanem, AM (2022). Parametric characterization, protectivity and potentiality of shallow hydrogeological units of a medium-sized housing estate, Shelter Afrique, Akwa Ibom State, Southern Nigeria. *Acta Geophys*. https://doi.org/10.1007-/s11600-022-00737-3

Evans, UF, George NJ, Akpan AE, Obot I.B., Ibot AN (2010). A study of superficial sediments and aquifers in parts of Uyo local government area, Akwa Ibom State, Southern Nigeria, using electrical sounding method. *Eur. J. Chem*. 2010; 7(3):1018–1022.

George NJ, Akpan AE, Evans UF (2016). Prediction of geohydraulic pore pressure gradient differentials for hydrodynamic assessment of hydrogeological units using geophysi-cal and laboratory techniques: a case study of the coastal sector of Akwa Ibom State, Southern Nigeria, *Arabian Journal of Geosciences* 9(4), 1-13

George NJ, Emah J.B, Ekong UN (2015a). Geohydrodynamic properties of hydrogeological units in parts of Niger Delta, southern Nigeria. *J. Afr. Earth Sci*., 105, 55- 63

George NJ, Agbasi OE, Umoh JA, Ekanem AM, Ejepu JS, Thomas JE, Udoinyang IE (2022b). Contribution of electrical prospecting and spatiotemporal variations to groundwater potential in coastal hydro-sand beds: a case study of Akwa Ibom State, Southern Nigeria, https://doi.org/10.1007/s11600-022-00994-2

George, NJ, Umoh, JA, Ekanem, AM, Agbasi, OE, Asfahani, J, Thomas, JE (2022a). Geophysical-laboratory data integration for estimation of groundwater volumetric reserve of a coastal hinterland through optimized interpolation of interconnected geo-pore architecture, J. Coastal Conservation, DOI : 10.1007/s11852-022-00902-2.

George, N J., Ibuot, JC, Ekanem AM, George AM (2018) Estimating the indices of inter-transmissibility magnitude of active surficial hydrogeologic units in Itu, Akwa Ibom State, southern, Arabian Journal Geosciences, Saudi Arabia, 11(6):1-16, DOI 10.1007/s12-517-018-3475-9.

George, NJ (2020). Appraisal of Hydraulic Flow Units and Factors of the Dynamics and Contamination of Hydrogeological Units in the Littoral Zones: A Case Study of Akwa Ibom State University and Its Environs, Mkpat Enin L.G.A, Nigeria. *Nat Resour Res.* 29, 3771–3788 https://doi.org/10.1007/s11053-020-09673-9

George, NJ, Akpan, AE and Ekanem, AM (2016). Assessment of textural variational pattern and electrical conduction of economic and accessible quaternary hydrolithofacies via geoelectric and laboratory methods in SE Nigeria: a case study of select locations in Akwa Ibom State. *Journal of Geological Society of India* 88(4), 517–528. Doi: 10.1007/s12594-016-0514-6.

George, NJ, Akpan, AE, Obot, IB (2010). Resistivity study of shallow aquifer in

parts of southern Ukanafun Local government area, Akwa-Ibom State. *Eur. J. Chem*., 7(3):693.

George, NJ, Ekanem, AM, Ibanga, JI, Udosen, NI, (2017). Hydrodynamic Implications of Aquifer Quality Index (AQI) and Flow Zone Indicator (FZI) in groundwater abstraction: A case study of coastal hydro-lithofacies in South-eastern Nigeria. *Journal of Coastal Conservation*. https://doi.org/10.1007/s1185-2-017-0535-3.

George, NJ, Ekanem, AM, Thomas, JE, Ekong SA (2021). Mapping depths of groundwater-level architecture: implications on modest groundwater-level declines and failures of boreholes in sedimentary environs. *Acta Geophys*. 69, 1919–1932 https://doi.org/10.1007/-s11600-021-00663-w

George, NJ, Emah JB, Ekong, UN (2015). Geophysical properties of hydrogeolo-gical units in parts of Niger Delta, southern Nigeria. *J. Afr. Earth Sci*. 105:55 – 63.

George, NJ, Ibanga, JI, Ubom, AI (2015a). Geoelectrohydrogeological indices of evidence of ingress of saline water into freshwater in parts of coastal aquifers of Ikot Abasi, southern Nigeria, Journal of African Earth Sciences, Egypt, 109, 37–46, http://dx.doi.org/10.1016/j.jafrearsci.-2015.05.001.

Ibanga, JI, George NJ, (2016). Estimating geohydraulic parameters, protective strength, and corrosivity of hydrogeological units: a case study of ALSCON, Ikot Abasi, Southern Nigeria. Arab J Geosci 9:363. https:// doi. org/ 10. 1007/ s12517- 016- 2390-1.

Ibuot JC, George NJ, Okwesili AN, Obiora DN (2019). Investigation of litho-textural characteristics of aquifer in Nkanu West Local Government Area of Enugu state, southeastern Nigeria. J Afr Earth Sci 153:197–207. https:// doi. org/ 10. 1016/j. jafre arsci. 2019. 03. 004

Ibuot, JC, Akpabio. GT George, NJ (2013). A survey of the repository of groundwater potential and distribution using geoelectrical resistivity method in Itu Local Government Area (L.G.A), Akwa Ibom State, southern Nigeria. *Central European Journal of Geosciences*, USA, 5(4), 538-547. DOI10.2478/s13533-012-0152-5.

Ibuot, JC, Ibuot, Okeke FN, George NJ, Obiora DN (2017). Geophysical and physicochemical characterization of organic waste contamination of hydrolithofacies in the coastal dumpsite of Akwa Ibom State, southern Nigeria, *Science & Technology: Water Supply*, 17 (6): 1626-1637, doi: 10.2166/ws.2017.066.

Ikpe, EO, Ekanem AM, George, NJ (2022). Modelling and assessing the protectivity of hydrogeological units using primary and secondary geo-electric indices: a case study of Ikot Ekpene Urban and its environs, southern Nigeria, *Modeling Earth Systems and Environment*. https://doi.org/10.1007/s40808-022-01366-x

Obianwu, VI, Chimezie I.C., Akpan AE, George, NJ (2011b). Estimation of Aquifer Secondary Parameter Distributions from Surficial Geophysical Measurements of Primary Parameters. A case Study of Ngor-Okpala Area of Imo State, *Journal of Applied Physics Research*, Canada, ISSN 1916-9639 (Print) ISSN 1916-9647 (online), 3(2), 67-80.

Obianwu, VI, George, George, NJ, Okiwelu, AA (2011d). Preliminary Geophysical Deduction of Lithological and Hydrological Conditions of the North-Eastern Sector of Akwa Ibom State, Southern Nigeria, *Research Journal of Applied Sciences, Engineering and Technology*, Vol. 3, No. 8, pp. 806-811.

Obianwu, VI, Chimezie, IC, Akpan AE, George, NJ (2011a). Surficial Geophysical Deduction of the Geomaterial and Aquifer Distribution at Ngor-Okpala Local Government Area of Imo State, Southern Eastern Nigeria. *Central European Journal of Geosciences*, USA, Doi: 10.2478/S13533-011-0011-0033-1. Vol.3 (4), 368-374

Obinawu, VI, George, NJ Udofia KM (2011c). Estimation of aquifer hydraulic conductivity and effective porosity distributions using laboratory measurements on core samples in the Niger Delta, Southern Nigeria. *International Review of Physics*, Praise worthy Prize, Italy 5 (1):19–24

Obiora, DN, Ibuot, JC, George NJ (2015a). Evaluation of aquifer potential, geoelectric and hydraulic parameters in Ezza North, southeastern Nigeria, uses geoelectric sounding. *Int J Sci Technol*. https:// doi. org/ 10. 1007/ s13762- 015-0886-y

Oladapo, MI, Mohammed MZ, Adeoye OO, Adetola BA (2004). Geo-electrical investigation of the Ondo state housing corporation estate Ijapo Akure, Southwestern Nigeria. *J Mining Geol* 40(1):41–48

Olubusola, IS, Daniel, AA, Oladimeji, OK (2018). Modeling of Groundwater Yield Using GIS and Electrical Resistivity Method in a Basement Complex Terrain, Southwestern Nigeria. *JGEESI*, 16(1): 1-17; Article no.JGEESI.42102

Singh, UK, Das, RK, Hodlur GK (2004). Significance of Dar-Zarrouk parameters in the exploration of quality affected coastal aquifer systems. *Environmental Geology*, 45, 696–702.

Tang, Y, Zhou, J, Yang, P, Yan, Zhou, N (2017). Groundwater Engineering (Springer Natural Hazards) 2nd ed.

Thomas, J. E, George N. J, Ekanem, A. M, Nsikak, E. E (2020). Electrostratigraphy and hydrogeochemistry of hyporheic zone and water-bearing caches in the littoral shorefront of Akwa Ibom State University, Southern Nigeria. *Environ Monit Assess.*, 192:505. https:// doi. org/ 10. 1007/ s10661- 020- 08436-6

Todd, D.K. (1980). Groundwater Hydrology, Second Edition, Wiley, New York

Udosen, NI, George NJ (2018a). A finite integration forward solver and a domain search reconstruction solver for electrical resistivity tomography (ERT), *Modeling. Earth System and Environment*, Switzerland, 4(1), 1-12, DOI 10.1007/s40808-018-0412-6

Udosen, NI, George, NJ (2018b). Characterization of electrical anisotropy in North Yorkshire, England using square arrays and electricl resistivity tomography, *Geomechanics and Geophysics for Geo-energy and Geo-resources*, Switzerland, 4(3), 215-233, https://doi.org/10.1007/s40948-018-0087-5

Umoh, JA, George, NJ, Ekanem, AM, and Emah, JB (2022) Characterization of hydro-sand beds and their hydraulic low units by integrating surface measurements and ground truth data

in parts of the shorefront of Akwa Ibom State, Southern Nigeria. *International Journal of Energy and Water Resources*. https://doi.org/10.1007/s42108-022-00215-y

Uwa, UE, Akpabio, GT, George, NJ (2019). Geohydrodynamic parameters and their implications on the coastal conservation: A case study of Abak Local Government Area (LGA), Akwa Ibom State, Southern Nigeria, *Nat Resour Res.*, Switzerland, 28(2), 349-367, https://doi.org/10.1007/s11053-018-9391-6

Venkateswaran S, Vijay, MP, Karuppannan S (2014). Delineation of groundwater potential zones using geophysical and GIS techniques in the sarabanga sub basin, Cauvery River, Tamil Nadu, India. *Int. J. Curr. Res. Acad. Rev.;* 2(1): 58–75.

Werner, AD, Bakker, M, Post, VE, Vandenbohede, A, Lu, C, Ataie-Ashtiani, B (2013). Seawater intrusion processes, investigation and management: Recent advances and future challenges. *Advances in Water Resources*, 51, 3-26.